Multiresolution SVD based Image Fusion

Dr. G.A.E. Satish Kumar[1], Jaya Krishna Sunkara[2]

[1]*Professor, Department of ECE, Vardhaman College of Engineering (Autonomous), Hyderabad, INDIA*
[2]*PG Scholar, Department of ECE, Sri Venkateswara University College of Engineering, Tirupati, INDIA*

Abstract: *Image fusion is the process of combining two or more images with specific objects with more precision. It is very common that when one object is focused remaining objects will be less highlighted. To get an image highlighted in all areas, a different means is necessary. This is done by the Image Fusion. In remote sensing, the increasing availability of Space borne images and synthetic aperture radar images gives a motivation to different kinds of image fusion algorithms. In the literature a number of time domain image fusion techniques are available. Few transform domain fusion techniques are proposed. In transform domain fusion techniques, the source images will be decomposed, then integrated into a single data and will be reconstructed back into time domain. In this paper, singular value decomposition as a tool to have transform domain data will be utilized for image fusion. In the literature, the quality assessment of fusion techniques is mainly by subjective tests. In this paper, objective quality assessment metrics are calculated for existing and proposed techniques. It has been found that the new image fusion technique outperformed the existing ones.*
Keywords: *Image fusion, Laplacian Pyramid, SVD, Wavelet.*

I. Introduction

Extracting more information from multi-source images is a gorgeous thing in remotely sensed image processing, which is called data fusion. There are many image fusion methods such as WS, PCA, WT, GLP etc. Among these methods WT and GLP methods can preserve more image spectral characteristics than the others. So here we adopt – wavelet method [1][2][3].
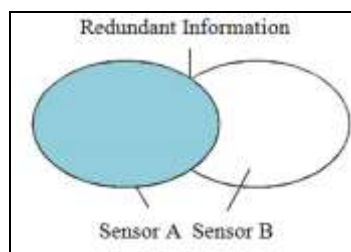

Fig. 1 Image Fusion

With the recent rapid developments in the field of sensor technologies multi-sensor systems have become a certainty in a growing number of fields such as remote sensing, medical imaging, machine vision and the military applications for which they were first developed [2]. Image fusion provides an effective way of reducing this increasing volume of information while at the same time mining all the useful information from the source images.Multi-sensor data often presents complementary information about the region charted, so image fusion delivers an effective method to enable comparison and analysis of such data. The role of image fusion apart from recognition is in applications such as remote sensing and medical imaging [4][5][6]. For example, visible-band and infrared images may be fused to aid pilots landing aircraft in poor visibility. Multi-sensor images often have different geometric representations, which have to be transformed to a common representation for fusion. Multi-sensor registration is also affected by the differences in the sensor images. However, image fusion does not necessarily imply multi-sensor sources, there are interesting applications for both single-sensor and multi-sensor image fusion system [7][8].

a. Single Sensor Image Fusion System

An illustration of a single sensor image fusion system is shown in Figure .The sensor shown could be a visible-band sensor such as a digital camera. This sensor captures the real world as a sequence of images [9]. The sequence is then fused in one single image and used either by a human operator or by a computer to do some task. For example in object detection, a human operator searches the scene to detect objects such intruders in a security area [10][11][12].
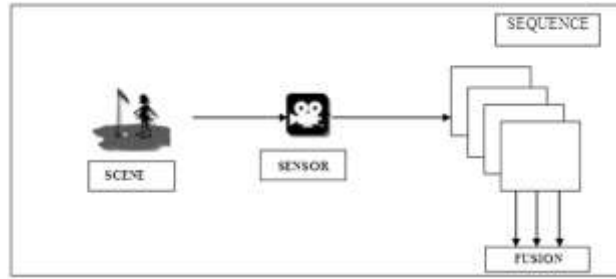
Fig. 2 Single-Sensor Image Fusion System

This kind of systems has some limitations due to the capability of the imaging sensor that is being used. The conditions under which the system can operate, the dynamic range, resolution, etc. are all limited by the capability of the sensor. For example, a visible-band sensor such as the digital camera is appropriate for a brightly illuminated environment such as daylight scenes but is not suitable for poorly illuminated situations found during night, or under adverse conditions such as in fog or rain [13].

b. *Multi-Sensor Image Fusion System*

Multi-sensor image fusion systems overcomes the limitations of a single sensor vision system by combining the images from these sensors to form a composite image Multiple images of same scene will be taken by two or more capturing devices and then be fused. It is sufficient to each capturing device to capture one image with better focus on one possible object. All the objects in the scene will be focused well, because of more capturing devices. The multi-sensor image fusion system is more efficient comparing to the single sensor image fusion system [14]. The multi sensor image fusion system is more accurate. The multi sensor image fusion system is shown in below figure. The multi sensor image fusion system is more robust and gives accurate results. Finally by comparing both single sensor image fusion system and multi sensor image system, the multi sensor image fusion system has more advantages.

c. *Performance Evaluation*

The performance of image fusion algorithms can be evaluated when the reference image is available. Here two performance metrics are considered. They are Peak signal to noise ratio (PSNR) and Root mean square error(RMSR)

$$PSNR = 20\log_{10} \frac{L^2}{\frac{1}{MN}\sum_{x=1}^{M}\sum_{y=1}^{N}(I_r(x,y) - I_f(x,y))^2}$$
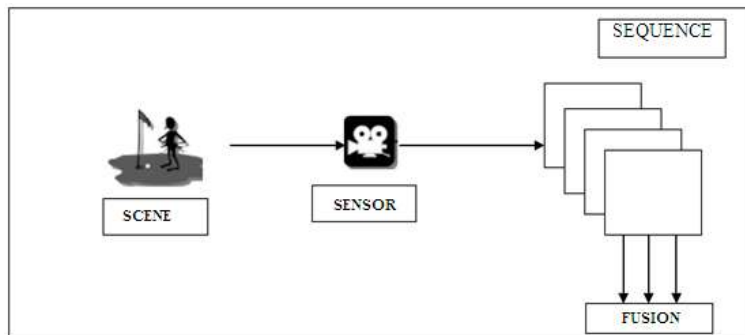

Fig. 3 Multi Sensor Image Fusion System

where, *L* in the number of gray levels in the image This value will be high when the fused and reference images are alike and higher value implies better fusion.

$$RMSE = \sqrt{\frac{1}{MN}\sum_{x=1}^{M}\sum_{y=1}^{N}(I_r(x,y) - I_f(x,y))^2}$$

It is computed as the root mean square error (RMSE) of the corresponding pixels in the reference image I_r and the fused image I_f. It will be nearly zero when the reference and fuse images are alike and it will increase when the dissimilarity increases [15].

II. Laplacian Pyramid based Image Fusion

This work focuses on both these requirements and proposes a method that integrates the Laplacian pyramid algorithm, wavelets and spatial frequency. Although the fusion can be performed with more than two input images, this study considers only two input images. The algorithm decomposes the input image using 2D-DWT. The lower approximations are subjected to Laplacian pyramid algorithm. The SF algorithm combined with wavelet fusion algorithm is used for higher approximations. The new sets of detailed and approximate coefficients from each image are then added to get the new fused coefficients.

The final step performs Inverse DWT with the new coefficients to construct the fused image. The two main components of the proposed algorithm are the Laplacian Pyramid algorithm and the wavelet algorithm and are explained in the following sub-sections. The Laplacian Pyramid [6] implements a —pattern selective approach to image fusion, so that the composite image is constructed not a pixel at a time, but a feature at a time. The basic idea is to perform a pyramid decomposition on each source image, then integrate all these decompositions to form a composite representation, and finally reconstruct the fused image by performing an inverse pyramid transform [16].

The first step is to construct a pyramid for each source image. The fusion is then implemented for each level of the pyramid using a feature selection decision mechanism. The feature selection method selects the most salient pattern from the source and copies it to the composite pyramid, while discarding the least significant salient pattern. In order to eliminate isolated points after fusion, a consistency filter is applied.
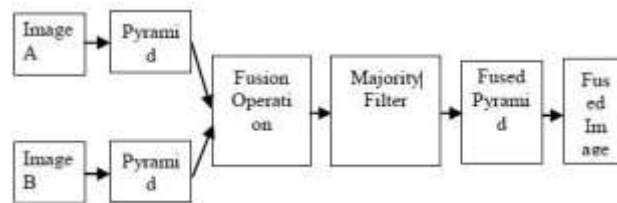
$$F_N(X,Y) = \frac{A_N(X,Y) + B_N(X,Y)}{2}$$

Fig. 4 Laplacian pyramid fusion algorithm

a. *Laplacian algorithm*

Main Function:
    Step 1:   IM← Read reference image.
               IM1← Read the first image.
               IM2← Read the second image.
    Step 2:   Apply the two input images to the fusion function which gives the resultant image.
    Step 3:   Calculate MSE and PSNR between the reference and resulting image.

Fusion Function:
Inputs: First image – IM1, Second image – IM2, Pyramid Levels – 2.
Output: Fused image.
    Step 1:   for i=1 to k
    Step 2:   IM ←reduced version of IM1 using DCT
    Step 3:   TEMP ← expanded version of IM using DCT
    Step 4:   Id1 ← IM1 – TEMP
    Step 5:   IM1 ← IM
    Step 6:   Repeat steps 2 to 5 for image 2.
    Step 7:   B ← [(Id1-Id2)≥0]
    Step 8:   Idf(i) ← Image with pixels from Id1 or Id2 whichever is high.
    Step 9:   end for
    Step 10:   imf = ½ (IM1 + IM2)
    Step 11:   for i=k to 1
    Step 12:   imf = Idf(i) + expand(imf)
    Step 13:   end for

Reduce Function:
Input: Image – I
Output: Reduced image – Ir
    Step 1:   mn← size(I)/2
    Step 2:   II ←dct(I)
    Step 3:   Ir←idct(II, 1 to mn, 1 to mn)

b. *Simulation results*

The two images to be fused are generated from the ground truth image using blurring as shown in Fig. 5 (top left). The aircraft in top half of the image is out of focus and the second aircraft is in focus. It is reverse in second image i.e. both images are contain complementary information. The fused and error (fused image subtracted from reference image) with 8 level pyramid are shown in Fig 5 (top right). The fused image is almost similar to reference image and the error image is almost zero. It shows that the fused image contains all information coming from the complementary source images.

Fig. 5 Laplacian pyramid fusion algorithm

III. Wavelet Based Image Fusion

Main function:
  Step 1: X=IM   - Reference image
  Step 2: X1=IM$_1$ - Read image 1
  Step 3: X2 = IM2 - Read image 2
Fusion function:
Inputs: First image – X1, Second image – X2, Decomposition level – 5
Output: Fused image
Step 1: Apply these two images to wavelet fusion function then we get result image.
Step 2: plot original and synthesized images
Step 3: Perform Wavelet decompositions
Step 4: Merge two images from their decompositions
Step 5: Restore the image using image fusion
Step 6: Using the wavelet and level menus, select the sym4 at level 5.
Step 7: From select fusion method frame, select the item max for both approximations and details.

a. *Simulation Results*

In wavelet technique we used two input images as shown in below Fig 6 (top left) and 6 (top right). Apply wavelet transform technique for two input images we get output image as shown in fig. 6 (bottom left) .Fused and error images are developed by using image fusion technique as shown in fig. 6 (bottom right).

Fig. 6 Screenshots of Image Fusion with wavelets

In comparison table in next section compare the design metrics of laplacian pyramid and wavelet transform technique. Wavelet transform gives high PSNR value 39.4951 and low RMSE value 7.3614.compare to laplacian pyramid wavelet gives better result. The performance metrics for evaluating the image fusion algorithms are shown in Table.

b. *Observations*

In this wavelet technique we observe both techniques are same but design metrics different. Laplacian gives low PSNR value 37.3154 and high RMSE value 12.1623 compare to wavelet transform. Wavelet transform gives high PSNR 39.4951 and low RSME 7.3614 .wavelet gives better result compare to laplacian.

IV. Multiresolution SVD

Multi-resolution singular value decomposition is very similar to wavelets transform, where signal is filtered separately by low pass and high pass finite impulse response (FIR) filters and the output of each filter is decimated by a factor of two to achieve first level of decomposition. The decimated low pass filtered output is filtered separately by low pass and high pass filter followed by decimation by a factor of two provides second level of decomposition.

$$X_1 = \begin{bmatrix} x(1) & x(3) & \bullet & \bullet & x(N-1) \\ x(2) & x(4) & \bullet & \bullet & x(N) \end{bmatrix}$$

Denote the scatter matrix $T_1 = X_1 X_1^T$ and let u_1 be the Eigen vector matrix that brings T_1 into diagonal metrics**.** Let $X = [x(1), x(2),..., x(N)]$ represent a 1D signal of length *N* and it is assumed that *N* is divisible by $2K$ for $K \geq 1$ 21-26. Rearrange the samples in such a way that the top row contains the odd number indexed samples and the bottom row contains the even number indexed samples. Let the resultant matrix called data matrix is:

The diagonal matrix $S_1^2 = \begin{matrix} S_1(1)^2 & 0 \\ 0 & S_2(1)^2 \end{matrix}$

contains the square of the singular values, with $S_1(1) > S_2(2)$.Let $X_1 = U_1^T X_1$ so that $X_1 = U_1 X_1$. The top row of 1 ˆ*X* , denoted 1 ˆ*X*(1,:) contains approximation component that corresponds to the largest eigenvalue. The bottom row of 1 ˆ*X*, denoted 1 *X*ˆ(2,:) contains detail component that corresponds to the smallest eigenvalue. Let 1 1 Φ = *X*ˆ (1,:) and 1 1 Ψ = *X*ˆ (2,:) represent the approximation and detail components respectively. The successive levels of decomposition repeats the procedure described above by placing the approximation component Φ1 in place of *X*. The above outlined procedure can be described formally. This procedure can be repeated recursively *K* times. Let Φ0(1,:) = *X* so that the initial approximation component is the original signal. For each level *l*, the approximation component vector Φ*l* has *l l N = N / 2* elements that are represented as:

The K-level MSVD for l=1,2,......k-1 as follows:

$$X_l = \begin{bmatrix} \phi_{l-1}(1) & \phi_{l-1}(3) & \bullet & \bullet & \bullet & \bullet & \phi_{l-1}(2N_{l-1}) \\ \phi_{l-1}(2) & \phi_{l-1}(4) & \bullet & \bullet & \bullet & \bullet & \phi_{l-1}(2N_l) \end{bmatrix}$$

$T_1 = X_1 X_1^T = U_1 S_1^2 U_1^T$, where singular values to be changed as $S_l(l) > S_l(2)$. $X_1 = U_1^T X_1$ $\phi_l = X_l(1,:)$ and $\varphi_l = X_l(2,:)$. In general, it is sufficient to store the lowest resolution approximation component vector ΦL, the details component vectors Ψl for $l = 1,2,...,L$ and the eigenvector matrices Ul for $=1,2,..., L$. Hence the MSVD can be written as: $X \rightarrow \{\phi_L, (\varphi_l)_{l=1}^2, (U_1)_{l=1}^2\}$. The original signal X can be reconstructed from the right hand side, since the steps are reversible. 1D multi-resolution singular value decomposition (MSVD) can be easily extended to 2D MSVD and even for higher dimensions. The first level decomposition of the image proceeds as follows. Divide the $M \times N$ image X into non-overlapping 2×2 blocks and arrange each block into a 4×1 vector by stacking columns to form the data matrix X_1.

The blocks may be taken in transpose raster scan manner or in other words proceeding downwards first and then to right. The Eigen-decomposition of the 4×4 scatter matrix is: $T 2 T 1 1 1 1 1 1 T = X X = U S U$ (12) where the singular values are arranged in decreasing order as $s1(1) \geq s2(2) \geq s3(3) \geq s4(4)$ Let $T 1 1 1 X^\wedge = U X$. The first row of $1 X^\wedge$ corresponds to the largest eigenvalue and considered as approximation component. The remaining rows contain the detail component that may correspond to edges or texture in an image. The elements in each row may be rearranged to form $M/2 \times N/2$ matrix.

Before proceeding to next level of decomposition, let $\Phi 1$ denote $M/2 \times N/2$ matrix formed by rearranging the row $1 \hat{X}(1,:)$ into matrix by first filling in the columns and then rows. Similarly, each of the three rows $1 X^\wedge(2,:)$, $1 X^\wedge(3,:)$ and $1 X^\wedge(4,:)$ may be arranged into $M/2 \times N/2$ matrices that are denoted as $1 \Psi V$, $1 \Psi H$ and $1 \Psi D$ respectively. The next level of decomposition proceeds as above where X is replaced by Φ_1.

The complete L level decompositions may be represented as: $X \rightarrow \{\phi_L, \{\varphi_1^V, \varphi_1^H, \varphi_1^D\}_{l=1}^L, \{U_1\}_{l=1}^L\}$

The original image X can be reconstructed from the right hand side, since the steps are reversible.

a. Algorithm

Main Function:
Step 1: IM ← Read reference image.
        IM1← Read the first image.
        IM2← Read the second image.
Step 2: Apply the two input images to the fusion function which gives the resultant image.
Step 3: [X1, U1] ← MSVD(IM1)
Step 4: [X2, U2] ← MSVD(IM2)
Step 5: Prepare LL, LH, HL and HH components (of an image say X) from the corresponding parts of the images X1 and X2 by using the following rule.
    i) For LL component take average of that of X1 and X2.
    ii) For the remaining components take from X1 or X2 whichever is high.
Step 6: U ← ½ (U1 + U2)
Step 7: imf← IMSVD(X, U)
Step 8: Calculate RMSE and PSNR between the reference and resulting image.

MSVD Function:
Input: Image – x
Outputs:MSVD coefficients – Y, Unitary matrix (U in SVD)
Step 1: m, n ← size(x)/2
Step 2: A← Zero matrix of order 4xm*n
Step 3: A ← x (reshape x into the format of x)
Step 4: [U,S] ←svd(x)
Step 5: T ← U*A
Step 6: Y.LL ← First row of T (reshaped into mxn matrix)
        Y.LH ← Second row of T (reshaped into mxn matrix)
        Y.HL ← Third row of T (reshaped into mxn matrix)
        Y.HH ← Fourth row of T (reshaped into mxn matrix)

IMSVD Function:
Inputs: MSVD coefficients – Y, Unitary matrix (U in SVD)
Output: Fused Image – X
Step 1: m, n ← size(Y.LL)
Step 2: mn← m*n
Step 3: T ← Zero matrix of order 4xm*n
Step 4: T ← Y (each of four components as rows, so that T is a matrix of order 4xm*n)
Step 5: A ← U*T
Step 6: X ← Zero matrix of order 2mx2n
Step 7: X ← A (by reshape)

b. Simulation Results

National Aerospace Laboratories (NAL) indigenous aircraft (SARAS), considered as a reference image *Ir* to evaluate the performance of the proposed fusion algorithm. The complementary pair input images *I*1 and *I*2 are taken to evaluate the fusion algorithm and these images are shown in Fig.7 (top left) and 7 (top right). Fig. (bottom left) shows fused images and Fig 7 (bottom right) shows the error images.

Fig. 7 Simulation Results with MSVD

It is observed that the fused images of both MSVD and wavelet are almost similar for these images. The reason could be because of taking the complementary pairs. One can see that the fused image preserves all useful information from the source images. The performance metrics for evaluating the image fusion algorithms are shown in Table I.

Table I Comparison of Three Methods

S.NO	METHODS	PSNR	RMSE
1	Laplacian Pyramid	37.314	12.1623
2	Wavelet Transform	39.4951	7.3614
3	MSVD	41.0605	5.1333

c. Observations

A novel image fusion algorithm by MSVD has been presented and evaluated. The performance of this algorithm is compared with well-known image fusion technique by Wavelets. Image fusion by MSVD performs almost similar to wavelets. It is computationally very simple and it could be well suited for real time applications. By observing the above table we show that MSVD gives better performance than wavelets.

V. Conclusions

A novel image fusion technique using DCT based Laplacian pyramid has been presented and its performance evaluated. It is concluded that fusion with higher level of pyramid provides better fusion quality. The execution time is proportional to the number of pyramid levels used in the fusion process. This technique can be used for fusion of out of focus images as well as multi-model image fusion. It is very simple, easy to implement and could be used for real time applications. Pixel-level image fusion using wavelet transform and principal component analysis are implemented in MATLAB. Different image fusion performance metrics with and without reference image have been evaluated. The simple averaging fusion algorithm shows degraded performance. Image fusion using wavelets with higher level of decomposition shows better performance. A novel image fusion algorithm by MSVD has been presented and evaluated. The performance of this algorithm is compared with well-known image fusion techniques. It is concluded that image fusion by MSVD perform almost similar to wavelets. It is computationally very simple and it could be well suited for real time applications. Moreover, MSVD does not have a fixed set of basis vectors like FFT, DCT and wavelet etc. and its basis vectors depend on the data set.

References

[1]   Pajares, Gonzalo & Manuel, Jesus de la Cruz, A wavelet based image fusion tutorial, *Pattern Recognition*, 37, 1855-872, 2007.

[2]   Varsheny, P.K., Multi-sensor data fusion, *Elec. Comm. Engg., Journal, 9(12), 245-53,* 1997.

[3]   Burt, P.J. & Lolczynski, R.J. Enhanced image capture through fusion, *Proc. of 4th International Conference on Computer Vision, Berlin, Germany, 173-82,* 1993.

[4]   Mallet, S.G. A theory for multiresolution signal decomposition: The wavelet representation. *IEEE Trans. Pattern Anal. Mach. Intel., 11(7), 674-93*, 1989.

[5]   Wang, H.; Peng, J. & W. Wu. Fusion algorithm for multi-sensor image based on discrete multiwavelet transform, *IEEE Pro. Vis. Image Signal Process*, *149(5)*, 2002.

[6]   Li, H.; Manjunath, B.S. & Mitra, S.K. Multisensor image fusion using wavelet transform, *Graph models image process, 5, 57(3), 235-45,* 2005.

[7]   Pu. T. & Ni, G. Contrast-based image fusion using discrete wavelet transform. *Optical Engineering, 39(8), 2075-2082,* 2000.

[8]   Yocky, D.A. Image merging and data fusion by means of the discrete two-dimensional wavelet transform. *J. Opt. Soc. Am. A, 12(9), 1834-841*, 1995.

[9]   Nunez, J.; Otazu, X.; Fors, O.; Prades, A.; Pala, V. & Arbiol, R. Image fusion with additive multiresolution wavelet decomposition: applications to spot1 landsat images. *J. Opt. Soc. Am. A, 16, 467-74*, 1999.

[10]   Rockinger, O. Image sequence fusion using a shift invariant wavelet transform. *Proceedings of IEEE Int. Conf. on Image Processing, 13, 288-91*, 1997.

[11]   Qu, G.H.; Zang, D.L. & Yan P.F. Medical image fusion by wavelet transform modulus maxima. *J. of the Opt. Soc. Of America*, *9, 184-90*, 2001.

[12]   Chipman, L.J.; Orr, T.M. & Graham, L.N. Wavelets and Image fusion. *Proceedings SPIE, 2529, 208-19,* 1995.

[13]   Jahard, F.; Fish, D.A.; Rio, A.A. & Thompson, C.P. Far/near infrared adapted pyramid-based fusion for automotive night vision. *IEEE Proc. 6th Int. Conf. on Image Processing and its Applications (IPA97), 886-90,* 1997.

[14]   Ajazzi, B.; Alparone, L.; Baronti, S. & Carla, R. Assessment pyramid-based multisensor image data fusion. *Proceedings SPIE, 3500, 237-48,* 1998.

[15]   Akerman, A. Pyramid techniques for multisensory fusion. *Proc. SPIE, 2828, 124-31,* 1992.

[16]   Toet, A.; Van Ruyven, L.J. & Valeton, J.M. Merging thermal and visual images by a contrast pyramid. *Optical Engineering*, *28(7), 789-92,* 1989.